
Vocabulary-Defined Semantics: Latent Space Clustering for Improving In-Context Learning

Jian Gu¹, Aldeida Aleti¹, Chunyang Chen², and Hongyu Zhang³

¹Monash University, jian.gu, aldeida.aleti@monash.edu

²Technical University of Munich, chun-yang.chen@tum.de

³Chongqing University, hyzhang@cqu.edu.cn

Abstract

In-context learning enables language models (LM) to adapt to downstream data or tasks by incorporating few samples as demonstrations within the prompts. It offers strong performance without the expense of fine-tuning. However, the performance of in-context learning can be unstable depending on the quality, format, or order of demonstrations, which in turn exacerbates the difficulty of optimization. Prior work, such as Knn Prompting, index samples based on the similarities of logits at the output-side, in addition to the regular retrieval operation at the input-side. They improve in-context learning by leveraging the core ability of next-token prediction, rather than relying solely on the emergent capacity to make analogies. Despite this, the hard-to-optimize issue of in-context learning still exists. In our view, it stems from the process of selecting demonstrations. To address this, we propose complementing in-context learning with an additional clustering operation. We propose a novel approach “vocabulary-defined semantics”. Grounded in LM vocabulary, which is the label space of model outputs, the proposed approach computes semantically equivalent latent representations for output labels. Then, taking the representations as centroids, a clustering operation is performed to align the semantic properties between the language model and the downstream data/tasks. Based on extensive experiments across diverse textual understanding datasets and multiple models, our approach outperforms the state-of-the-art in terms of effectiveness and efficiency. On average, it achieves 3% – 49% improvements while requiring only half of the computation time.

1 Introduction

Language models (LMs) are drawing significant attention due both to their potential opportunities and associated risks [1]. Despite demonstrating impressive performance, in some scenarios, it may not be convenient to finetune them to downstream data/tasks, such as Language Model-as-a-Service (LMaaS) [2]. As a solution, in-context learning [3] serves as an effective approach to utilizing language models for downstream tasks. Unlike model fine-tuning, in-context learning adapts to downstream data or tasks by incorporating demonstrations into the prompts. Using the emerging ability to draw analogies from demonstrations [4], it offers strong performance without the expense associated with model fine-tuning.

However, in-context learning is not a stable technique and may be affected by multiple factors, which exacerbates the difficulty of further optimization. For example, the performance may be affected by the quality of demonstrations [5, 6], their format [7, 8], and even their order [9, 10]. The state-of-the-art (SOTA) KNN prompting [11] takes a significant step forward. Rather than solely depending on the emergent ability of language models to make analogies, the solution also utilizes the core capability of next-token prediction to enhance in-context learning. In addition to the retrieval

Preprint. Under review.

operation of selecting demonstrations at the input-side, it introduces an additional indexing operation to support KNN decision at the output-side. The limitations are, while using the indexed data as the reference in KNN decision, it cannot cooperate with the normal LM inference. Also, it cannot handle the case where the samples corresponding to a specific output label are unavailable.

Nevertheless, the critical issue of in-context learning still exists. In our view, it is caused by the drawbacks of selecting demonstrations (also applies to the case of composing demonstrations). First, in-context learning retrieves only a subset from all useable demonstrations, so the retrieval operation tends to be a suboptimal option, since it is unclear which samples would be the best choices. Second, assume the best samples to retrieve can be known beforehand, the retrieval operation is still suboptimal, since the best samples may not be included in the retrievable samples. To solve the issue of difficult optimization, we complement in-context learning with an additional clustering operation, and define a clear objective for performance optimization. Similar to SOTA KNN Prompting [11], our focus is on the output-side, not the input-side. Meanwhile, we replace its indexing operation with a clustering operation that aligns semantic properties, to overcome the limitations.

We propose a novel and effective approach: *Vocabulary-Defined Semantics*, short for *VDS*. Grounded in LM vocabulary, which is the label space of model outputs, we compute the semantically equivalent latent representations for all output labels. Then, we determine the logits directly in latent space (which is disentangled for latent representations), and use the logits to quantify the semantic gap between the language model and downstream data, so we will know on the fly how good the latent representations are. Last, taking the representations as centroids, we cluster the representations of downstream data to mitigate their semantic gap with the language model. By defining semantic bases of the label space, computing disentangled logits to quantify the semantic gap, and clustering representations to optimize the logits, our approach incorporates KNN decisions into LM inference. It aggregates the semantic information from the downstream data and cooperates with LM inference.

In addition, we have conducted large-scale experiments and detailed analysis across diverse datasets of text understanding, with four model families: GPT2 (0.13B-1.61B) [12], Qwen2 (0.49B-7.62B) [13], Gemma2 (2.61B-9.24B) [14], and Llama3 (8.03B) [15]. Based on our results, our approach outperforms the SOTA in both effectiveness and efficiency. On average, our approach obtains 3% – 49% improvements, while taking only half computation time. The replication repository is attached as supplementary material.

Our contributions are as follows:

- We define a collection of specialized representations, termed “semantic bases” for disentangled semantics. It allows for more precise alignment of semantic properties during tasks like language model inference, leading to improved performance and stability.
- We propose a novel way to compute logits via similarity measurement instead of common matrix multiplication, leveraging the local isotropy of LM latent space. The logits can be used to quantify the semantic gap between the language model and downstream data.
- We implement representation clustering through a lightweight neural clustering module. The clustering operation aligns the semantic property of the language model with downstream data. It benefits the performance of in-context learning while reducing the computation cost.

2 Background

2.1 In-Context Learning

In-context learning (ICL) is a prompting paradigm of language models. It retrieves samples and includes them as demonstrations in the prompts, to let models learn from the analogy [3]. In the basic usage of language models, a model shall predict an output y for the given input x . In contrast, ICL will retrieve samples from a corpus of all useable input-output pairs, to obtain a collection $\mathcal{T} = \{(x_i, y_i)\}$. The retrieved samples will be filled in templates $\pi(x_i, y_i)$ and concatenate with the given input x as a prompt: $\pi(x_1, y_1) \oplus \pi(x_2, y_2) \oplus \dots \oplus \pi(x_{|\mathcal{T}|}, y_{|\mathcal{T}|}) \oplus \pi(x, *)$. Then, the model will turn to predict an output y for the constructed prompt. Benefit from the emergent abilities of large-scale LMs, the use of in-context learning can avoid the expensive cost of model finetuning, while obtaining the equivalent performance in the adaptation to downstream data or tasks.

2.2 Entanglement and Disentanglement

Entanglement indicates the phenomenon where the elements of a vector data correlate with each other. In contrast, disentanglement means that the elements are independent of each other [16]. For example, LM latent representations, namely distributed representations (such as [0.1, 0.3, 0.4, 0.2]), are entangled while onehot embeddings (such as [0, 0, 1, 0]) are disentangled.

Following the definitions, for the representations in latent space, the logits computed on the vocabulary is entangled. Recall the computation in language models, in the forward-pass, the logits is computed on LM vocabulary and compared with the ground truth to obtain the loss. Then, in the backward-pass, the loss is backpropagated to model layers to obtain the gradients for model parameters. The dimension size of latent space is smaller than the vocabulary size, and the change in dimension size indicates the meaning of each element is no longer independent, which indicates an entanglement. Therefore, the logits is entangled for LM latent space even though disentangled for LM vocabulary. The entanglement is caused by the dimension transformation, namely the LM-head matrix.

Entanglement tends to restrict the potential improvements in efficiency and robustness. An entangled logits cannot represent a clear and intuitive meaning in latent space, which will cause challenges to further optimization. On efficiency, the dimension transformation via a huge LM-head matrix is mandatory in logits computation, so it is hard to reduce the costly computation; On robustness, the entangled logits will be sensitive to the absolute numerical magnitude of latent representations, which damages flexibility. Or else, the precision may not be guaranteed. In this paper, leveraging the disentangled logits, our approach obtains breakthroughs on these restrictions.

3 Vocabulary-Defined Semantics

Our approach defined and utilized the semantics of LM latent space, leveraging the vocabulary, as illustrated in Figure 1. We name our approach *Vocabulary-Defined Semantics*, short as *VDS*. In *VDS*: (1) First, we obtain the semantically equivalent latent representations of vocabulary labels by solving the pseudoinverse of the LM-head matrix, termed as “semantic basis”. Semantic bases faithfully represent the label space of model outputs and can cover all output labels in the vocabulary; (2) Then, based on the local isotropy of LM latent space [17], we can compute logits by measuring the similarities between latent representations and semantic bases. The novel practice of logits computation is directly in the latent space. Therefore, the computed logits is disentangled to latent representations, and can be used to quantify the semantic gap between the language model and downstream data; (3) Further, taking semantic bases as centroids, we perform centroid-known clustering on the latent representations of useable samples. The clustering operation can optimize the logits and mitigate the semantic gap of the language model with the downstream data.

3.1 Vocabulary-defined Semantic Fields

In the common way of logits computation, the data representation is projected to the LM vocabulary, and its actual semantic meaning is represented by the probability distribution on the vocabulary. Given this, we use the vocabulary to define the semantic property of LM latent space. Considering onehot embeddings are the most semantically representative distributions in the vocabulary, we compute the corresponding latent representations as the semantically equivalents of vocabulary labels. Since the softmax operation maintains monotonicity, onehot embeddings shall be regarded as logits.

For a given LM-head matrix, we conduct matrix multiplication to get the corresponding representation in the latent space. Since the computation direction is from logits to representations, instead of using the LM-head matrix \mathbb{W} , we use its pseudoinverse \mathbb{W}^+ . If there are v labels in the vocabulary, there will be v unique semantic bases representing all semantic meanings. At the output side of LM, we multiply each onehot embedding \vec{e} by the pseudoinverse matrix \mathbb{W}^+ to obtain the corresponding representation \vec{s} . That is, $\vec{s} = \vec{e} \cdot \mathbb{W}^+$. The computation is equivalent to solving the least squares problem of a system of linear equations. We call each of the obtained vectors *semantic basis*.

3.2 Similarity-based Semantic Logits

We directly determine the logits in the LM latent space, not on the vocabulary. In common practice, the logits are computed *after* the LM-head. In the LM forward-pass, the logits is obtained by the

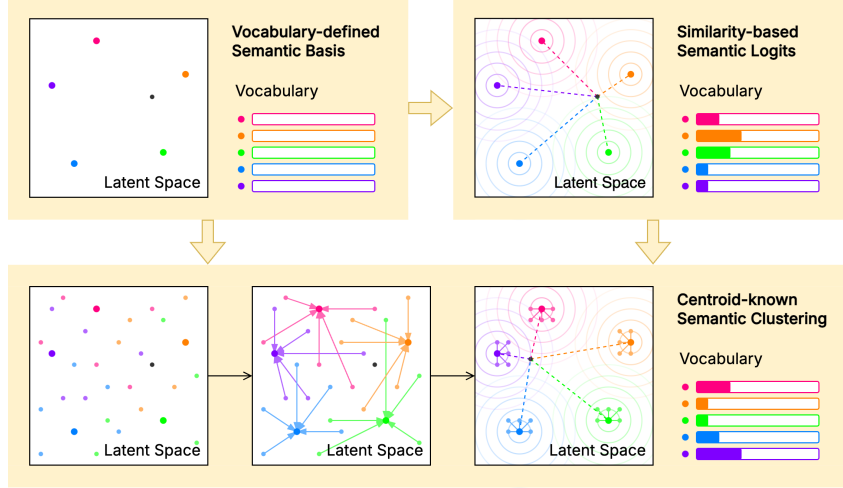


Figure 1: We illustrate with an LM, where the vocabulary consists of five colorful labels: (1) On the semantic basis (upper-left), we obtained the semantic bases in the latent space, represented by large color dots. The colors correspond to the labels in the vocabulary one to one; (2) On the semantic logits (upper-right), the small dark dot means the representation of arbitrary data. We measure its similarities with the semantic bases as logits. The logits are normalized as probabilities on the vocabulary, and the argmax label is *orange*; (3) On the semantic clustering (bottom), small color dots mean the representations of useable samples, and their colors indicate the corresponding ground truth. Originally, they were mixed and scattered all around. By clustering, they are gathered by color and into clusters centered in semantic bases. The clustering operates on the latent space, affecting the dark dot as well. The logits of the dark has changed, and its argmax label becomes *violet*.

multiplication between the last-layer latent representation and the LM-head matrix, and then is compared with the ground truth to compute the loss. Further, in the backward-pass, the loss will propagate the gradients back from the LM-head to the embeddings layer. In our approach, the logits is obtained *before* the LM-head. We use the similarity between latent representation and semantic bases to compute the logits. The similarity-based logits is disentangled to latent representations. It becomes intuitive than the disentangled logits, and will support further operations.

The latent space of Transformer models is proved to be locally isotropic [17], in terms of information and semantics. Therefore, we can compute logits in latent space by measuring the distances between representations, as an alternative to the typical way of matrix multiplication on the vocabulary. Isotropy means that the properties of a space are uniform in all directions. That is, in different directions of the latent space, the semantic differences of representations in the same distance remain close. Therefore, when we consider all semantic bases, instead of only one basis, the hypothesis is almost true that *the similarity of representations in the latent space remains positively correlated with the similarity of the corresponding distributions on the vocabulary*.

Algorithm 1 Similarity-based Semantic Logits

Require: n semantic bases \vec{b}_i ; representation \vec{r}
Ensure: probability distribution $probs$
 $logits \leftarrow \text{init_1d_tensor}(n)$
for $i \leftarrow 0$ **to** $n - 1$ **do**
 $logits[i] \leftarrow \text{similarity_metric}(\vec{b}_i, \vec{r})$
end for
 $probs \leftarrow \text{softmax}(logits)$

Similarity-based Semantic Logits. For a given representation, the logits is commonly computed by multiplying with the LM-head matrix, a novel practice is to compute its projection to the semantic bases using cosine similarity. Leveraging the positive correlation between the representation similarity in the latent space and the distribution similarity on the vocabulary, we compute the logits based on their similarities with the semantic bases. The similarity metric tends to be the cosine similarity, so

the logits indicate the projections to the semantic bases. Further, the logits can be used to compute the probability distribution on the vocabulary, as shown in Algorithm 1.

Based on similarity-based logits, the difference between the normal LM inference and KNN decision can be reformulated as the semantic gap of semantic bases (namely the language model) and downstream data. The effect of similarity-based logits is equivalent to that in normal LM inference. Taking the downstream data to replace semantic bases in logits computation, the effect of logits will make LM inference similar to KNN decision. The difference in results of normal LM inference and KNN decision indicates a semantic gap. Further, by mitigating the semantic gap, we will incorporate KNN decisions into LM inference to guarantee the adaptation of in-context learning.

3.3 Centroid-known Semantic Clustering

The semantic gap of KNN decision to the normal LM inference can be explained as, the semantic logits of downstream data cannot correspond to the ground truth. As a solution, we cluster the representations of downstream data in the last-layer latent space, to let them be closer to the ground truth, namely the corresponding semantic bases. Through centroid-known clustering on downstream data, the logits can quantify the semantic gap between the language model and the downstream data. The objective of clustering is to optimize the logits, that is, mitigating the semantic gap.

We specify each semantic basis as the centroid of each cluster. In the optimal situation, the last-layer representations of the same semantic meaning (corresponding to the same label), should stay in the same cluster. It can be taken by non-neural methods. We adopt a learning-based neural clustering method, so we can study more on similarity-based logits (in Section 5).

$$\lambda(\vec{r}) = \text{LN}(\text{MLP}(\vec{r} \odot \text{CA}(\vec{r}))) \quad (1)$$

$$\text{CA}(\vec{r}) = \text{Bn}(\text{avg}(\vec{r})) + \text{Bn}(\text{max}(\vec{r})) \quad (2)$$

We introduce a simple neural clustering module for semantic clustering, which consists of a channel attention (CA), a multi-layer perceptron (MLP), and a layer normalization (LN), as shown in Equation (1). The channel attention learns the coefficients of the representations, based on the information in the channel domain [18], as shown in Equation (2). The coefficients are a sum of the Bottleneck (Bn) outputs, respectively on the average-pooling (avg) and the maximum-pooling (max) of representations. Meanwhile, MLP and LN learn non-linear transformations in the latent space.

Logits-Numerical Sensitivity. In latent space clustering, whether the logits is entangled will affect the performance. A disentangled logits shall indicate a more robust logits-numerical sensitivity. We use the term to describe the sensitivity of loss computation to the numeric values of logits.

4 Experiments

In the following, we will introduce the experimental setup, and discuss the results on the effectiveness and efficiency. Following the prior work of in-context learning, the experiments are conducted with a wide range of model scales on diverse datasets, as shown in Table 1 and Table 2. On the results, the optimal scores are stressed with gray color.

	GPT2				Qwen2			Gemma2		Llama3
	Small	Medium	Large	XL	0.5B	1.5B	7B	2B	9B	8B
Parameters	137M	380M	812M	1.61B	494M	410M	7.62B	2.61B	9.24B	8.03B
Num. of Layer	12	24	36	48	24	28	28	26	42	32
Dimension Size	768	1,024	1,280	1,600	896	1,536	3,584	2,304	3,584	4,096
Vocabulary Size	50,257				151,936		152,064	256,000		128,256

TABLE 1: Stats of Language Models. We use recognized open-source LMs and involve four model families in our experiments: GPT2 (0.13B-1.61B) [12], Qwen2 (0.49B-7.62B) [13], Gemma2 (2.61B-9.24B) [14], and Llama3 (8.03B) [15].

		AGNews	CARER	MR	MRPC	SST5	SUBJ	TREC	WebSS
Num. of Classes		4	6	2	2	5	2	6	8
Class Balance		✓	✗	✓	✗	✗	✓	✗	✗
Avg. Length of Prompts		59.2	26.1	31.9	63.2	29.0	34.1	16.4	29.9
Num. of Data	Train	120,000	16,000	8,662	4,076	8,544	8,000	5,452	10,060
	Test	7,600	2,000	2,000	1,725	2,210	2,000	500	2,280
Num. of Shots	1k-context	2	4	8	4	4	8	8	2
	2k-context	4	8	16	8	8	16	16	4

TABLE 2: Stats of Datasets, and Number of Allowed Shots in the Prompts. We conduct evaluations with established text understanding tasks, respectively for text classification: AGNews [19], SUBJ [20], TREC [21], and WebSS [22]; sentiment analysis: MR [23] and SST5 [24]; emotion recognition: CARER [25]; as well as similarity detection: MRPC [26].

4.1 Setup

Baselines. In our experiments, we study the effects of semantic clustering on general in-context learning, short as ICL [27]. Besides, we compare with the SOTA in-context learning method, *KNN* prompting, short as KP [11]. We reproduce the practice of ICL and KP following the paper [11]. As an extension of the study, we also compare with parameter-efficient finetuning methods, including LORA [28] and IA³ [29].

Metrics. We follow the common practice, using *accuracy* to evaluate balanced datasets, and *F1* to evaluate imbalanced datasets. The reason is that, accuracy is preferred for its simplicity and directness, while F1 shall be taken when the precision-recall trade-off is a concern.

Environments. Our implementation is based on PYTORCH [30] and TRANSFORMERS [31]. The experiments are conducted on Nvidia V100 GPU (32 GB). In the experiments with Qwen2, Gemma2, and Llama3 models, we apply INT4 quantization to reduce the memory cost (while maintaining the model performance) [32, 33]. The LM quantization is dependent on the PEFT¹ library. GPT2 models are loaded without quantization.

4.2 Pipelines

We use few-shot prompts for in-context learning methods, making full use of the allowed context length. The prompt templates used in our experiments are available in Appendix A. For ICL, we retrieve the demonstrations randomly from the training set, and keep the number of demonstrations the same for each class. For KP, the retrieval operation is the same. The additional indexing operation follows the official implementation, which is based on KL divergence. The downstream data that is more similar in the probability distribution are more likely to be retrieved. For PEFT methods, we use zero-shot prompts to reduce the effects of in-context prompting. Meanwhile, we specify the recommended modules as trainable based on their papers. That is, the QKV matrices in LORA are trainable; QKV matrices plus the second FC layer in IA³) are trainable.

4.3 Effectiveness Study

Based on the results shown in Table 3, on average, VDS shows the optimal performance, while KP shows the suboptimal performance, both are better than ICL. Comparing the improvements of VDS on different language models, the improvements on Gemma2 models are most significant, which are 44% and 49%; while the improvements on Llama3 are marginal, which is 3%. The mean value of average improvements is 15.3%. The difference is mainly decided by the parameter amount of language models. By comparing the models of similar size (namely Qwen2-7B, Gemma2-9B, and Llama3-8B), where Gemma2-9B has a doubled vocabulary size to Llama3-8B, we may conclude that a large vocabulary size indicates better improvements. It fulfills the intuition, since a large vocabulary indicates the semantic meanings can be better distinguished via clustering. In other words, when the vocabulary is larger, the existing methods are more likely to underperform while our “vocabulary-defined semantics” tends to show better advantages. In contrast, the dimension size is not a critical factor since the difference is marginal, so the high-dimensional property of latent space shall be very similar. In addition, the quality of latent representations in different models also matters.

¹<https://github.com/huggingface/peft>

Dataset	Method	GPT2				Qwen2			Gemma2		Llama3	Avg.
		Small	Medium	Large	XL	0.5B	1.5B	7B	2B	9B	8B	
AGNews (Acc.)	ICL	0.302	0.571	0.533	0.752	0.816	0.802	0.809	0.250	0.250	0.876	0.596
	KP	0.867	0.875	0.869	0.874	0.866	0.883	0.892	0.258	0.250	0.898	0.753
	VDS	0.918	0.924	0.928	0.928	0.903	0.938	0.939	0.907	0.907	0.940	0.923
CARER (F1)	ICL	0.133	0.086	0.130	0.098	0.229	0.337	0.484	0.053	0.092	0.371	0.201
	KP	0.323	0.322	0.317	0.283	0.518	0.466	0.477	0.136	0.075	0.500	0.342
	VDS	0.613	0.607	0.589	0.643	0.738	0.680	0.700	0.653	0.630	0.627	0.648
MR (Acc.)	ICL	0.501	0.500	0.705	0.526	0.843	0.907	0.936	0.500	0.500	0.936	0.685
	KP	0.730	0.723	0.831	0.843	0.852	0.900	0.924	0.497	0.500	0.923	0.772
	VDS	0.810	0.855	0.859	0.866	0.852	0.903	0.929	0.737	0.726	0.906	0.844
MRPC (F1)	ICL	0.399	0.399	0.399	0.399	0.399	0.399	0.399	0.399	0.399	0.399	0.399
	KP	0.543	0.515	0.586	0.558	0.608	0.676	0.695	0.489	0.251	0.609	0.553
	VDS	0.620	0.627	0.631	0.633	0.615	0.729	0.785	0.616	0.605	0.641	0.650
SST5 (F1)	ICL	0.082	0.158	0.075	0.149	0.308	0.404	0.485	0.115	0.114	0.351	0.224
	KP	0.322	0.356	0.382	0.384	0.398	0.450	0.482	0.175	0.089	0.447	0.349
	VDS	0.392	0.451	0.436	0.459	0.441	0.483	0.526	0.347	0.369	0.456	0.436
SUBJ (Acc.)	ICL	0.500	0.501	0.502	0.559	0.670	0.930	0.843	0.500	0.500	0.933	0.644
	KP	0.807	0.868	0.889	0.900	0.853	0.940	0.940	0.525	0.500	0.947	0.817
	VDS	0.914	0.923	0.931	0.945	0.927	0.952	0.959	0.894	0.905	0.961	0.931
TREC (F1)	ICL	0.472	0.414	0.572	0.436	0.772	0.718	0.861	0.053	0.038	0.787	0.512
	KP	0.818	0.816	0.872	0.833	0.850	0.901	0.914	0.089	0.157	0.873	0.712
	VDS	0.896	0.924	0.916	0.914	0.907	0.925	0.943	0.890	0.894	0.892	0.910
WebSS (F1)	ICL	0.245	0.132	0.096	0.209	0.349	0.397	0.415	0.034	0.029	0.436	0.234
	KP	0.704	0.712	0.628	0.705	0.775	0.832	0.805	0.102	0.029	0.835	0.613
	VDS	0.796	0.806	0.793	0.803	0.785	0.815	0.836	0.731	0.727	0.828	0.792
Avg.	ICL	0.329	0.345	0.377	0.391	0.548	0.612	0.654	0.238	0.240	0.636	0.437
	KP	0.639	0.648	0.672	0.673	0.715	0.756	0.766	0.284	0.231	0.754	0.614
	VDS	0.745	0.765	0.760	0.774	0.771	0.803	0.827	0.722	0.720	0.781	0.767

TABLE 3: Performance on Text Understanding with In-Context Learning Methods.

Meanwhile, as shown in Table 3, compared with ICL and KP, our approach shows huge improvements in CARER, TREC, and WebSS datasets, which are 45%, 40% and 56% compared to ICL meanwhile 31%, 20% and 18% compared to KP; then show moderate improvements in AGNews and SUBJ datasets; and last show slight advantages in MR, MRPC, and SST5 datasets. The degree of improvements varies on datasets while the causes are not the obvious factors in the experiments, such as the number of shots in the prompts, the amount of useable downstream data, etc. Instead, the improvements are mainly affected by the task. In text classification and emotion recognition (CARER), our “vocabulary-defined semantics” can show great advantages over others; but in sentiment analysis (MR, SST5) and similarity detection (MRPC), the improvements seem not that obvious. Based on the details of datasets, the output labels in MR are easy to distinguish while in SST5 are challenging. Therefore, for MR, ICL and KP are good enough so the space for improvements is small; while for SST5, the quality of latent representations may not be that good, therefore, the scores on SST5 are the lowest. In addition, MRPC requires the reasoning ability of language models, which explains why the improvements are not that good. Our semantic-based approach is dependent on the quality of latent representations, this is the reason why VDS performs better on other datasets.

Method	AGNews (Acc.)	CARER (F1)	MR (Acc.)	MRPC (F1)	SST5 (F1)	SUBJ (Acc.)	TREC (F1)	WebSS (F1)	Avg.
LoRA	0.272	0.075	0.500	0.399	0.075	0.842	0.430	0.174	0.346
IA ³	0.941	0.889	0.944	0.727	0.464	0.979	0.940	0.916	0.850
ICL	0.876	0.371	0.936	0.399	0.351	0.933	0.787	0.436	0.636
KP	0.898	0.500	0.923	0.609	0.447	0.947	0.873	0.835	0.754
VDS	0.940	0.627	0.906	0.641	0.456	0.961	0.892	0.828	0.781

TABLE 4: Performance on Text Understanding with Llama3-8B with PEFT methods.

Based on the results shown in Table 4, in-context learning methods, including our approach, perform better than LORA but worse than IA³. It indeed indicates a performance gap between in-context learning methods and finetuning methods, while the gap is accompanied by the additional computation cost, as well as the suitability in different usage scenarios. Besides, the reason why LORA shows bad performance is because LORA only finetune the self-attention module but the feed-forward module tends to be the better choice in model adaptation [34, 35, 36].

4.4 Efficiency Study

On the computation cost, KP requires the most, then PEFT methods, while ICL and VDS require the least. As shown in Table 5, based on the average time cost, ICL is the fastest and only costs around 1.3 hours. Then, VDS and KP take 2.3 and 5.4 hours respectively, while LoRA and IA³ cost around 3.6 hours. The INFERENCE operation of in-context learning methods takes longer time, since ICL and KP are using few-shot prompts, and the prompts occupy the 1k-context (GPT2 LMs) and 2k-context (Pythia LMs). In contrast, PEFT methods and VDS take zero-shot prompts so their inference is faster. Except from ICL, besides INFERENCE, all methods have an additional operation. The indexing operation of KP finds high-quality demonstrations for few-shot prompting by analyzing the logits and the ground truth of training data. It consists of a forward-pass with few-shot prompts and the ranking of neighboring logits (measured by KL divergence). PEFT methods require LM forward-pass and backward-pass with zero-shot prompts, the amount of trainable parameters is small but the computation cost of backpropagation cannot be reduced. In contrast, VDS requires LM forward-pass but the backward-pass with zero-shot prompts is only on the neural clustering module. The clustering operation of VDS is on useable downstream data, since the data amount of AGNews is larger than other datasets, the time cost of clustering on AGNews is greatly larger than on other datasets. In addition, due to the disentanglement, the time cost of logits computation can be further reduced to $1/v$ by merely optimizing with the ground truth, without damaging the performance.

Method	Operation	AGNews	CARER	MR	MRPC	SST5	SUBJ	TREC	WebSS	Avg.
LoRA	Training	19.776	2.112	1.205	0.693	1.152	1.123	0.679	1.336	3.510
	Inference	0.440	0.093	0.098	0.104	0.108	0.100	0.023	0.107	0.134
IA ³	Training	19.605	2.095	1.190	0.685	1.144	1.118	0.673	1.328	3.480
	Inference	0.437	0.092	0.098	0.104	0.105	0.099	0.023	0.107	0.133
ICL	Inference	3.471	1.408	1.020	0.908	1.278	1.051	0.395	1.205	1.342
KP	Indexing	2.067	3.279	1.114	1.075	2.954	1.063	3.800	3.773	2.391
	Inference	8.841	3.005	1.744	1.486	3.027	1.709	0.776	3.864	3.056
VDS	Clustering	11.370	1.405	0.766	0.405	0.754	0.711	0.477	0.881	2.096
	Inference	0.261	0.176	0.176	0.168	0.193	0.176	0.043	0.199	0.174

TABLE 5: Runtime on Text Understanding with Llama3-8B (in Hours).

On the storage cost, KP requires the most storage cost while PEFT methods and VDS have much lower costs. For a given language model, assume its dimension size of latent representations is d , the number of LM layers is l , and the size of LM vocabulary is v . ICL has no additional storage. KP needs to store the logits of neighboring prompts from the useable data, for each label in the vocabulary, that is, $k * v * v$ when the number of nearest neighbors is k . As PEFT methods, LoRA and IA³ store the additional trainable parameters. Taking their recommended setups, the amount of their parameters are $4 * r * d * l$ and $7 * d * l$, when the low-rank parameter is r . For our approach VDS, the storage cost is the neural clustering module, that is, $\frac{33}{8} * d * d$. The number of trainable parameters consists of $4 * d * d$ for MLP and $\frac{1}{8} * d * d$ for CA. It can be further reduced to $\frac{33}{8} * d$ via parameterized hypercomplex multiplication [37].

5 Analysis and Explanation

In the following, we take an ablation study to further discuss similarity-based logits computation. It is centered on the effects of logits on the performance, when taking different practices of logits computation in clustering or inference operations. We will discuss more on logits disentanglement as well. The experiments are conducted on the same textual datasets, using Llama3-8B model. We use labels in the form of VDS[CLUSTER][INFER] to distinguish different settings, where CLUSTER and INFER indicate the practice of logits computation in clustering or inference operations.

Logits Computation. We include VDS as the baseline, marked as VDS[sm][sm], where the similarity-based logits computation (short as sm) is used in both operations of inference and clustering. By comparing with the common way of using matrix multiplication (short as mm) for logits computation in inference, we can see how similarity-based logits make effects in forward-pass, so prepare such a variant VDS[sm][mm]; By comparing with the common logits computation in clustering, we can see how similarity-based logits differ in backward-pass, prepare such a variant VDS[mm][sm]. Meanwhile,

Category	Variant	AGNews (Acc.)	CARER (F1)	MR (Acc.)	MRPC (F1)	SST5 (F1)	SUBJ (Acc.)	TREC (F1)	WebSS (F1)	Avg.
	VDS [sm] [sm]	0.940	0.627	0.906	0.641	0.456	0.961	0.892	0.828	0.781
Inference	VDS [sm] [mm]	0.940	0.627	0.906	0.641	0.459	0.960	0.892	0.830	0.782
Clustering	VDS [mm] [sm]	0.934	0.645	0.906	0.647	0.449	0.964	0.914	0.804	0.783
	VDS [sm-gt] [sm]	0.939	0.653	0.912	0.661	0.456	0.965	0.916	0.819	0.790
Disentangle	VDS [mm-exp] [sm]	0.250	0.086	0.500	0.399	0.075	0.500	0.038	0.029	0.235
	VDS [sm-exp] [sm]	0.940	0.640	0.909	0.638	0.437	0.953	0.906	0.805	0.779

TABLE 6: Performance of Ablation Study with Llama3-8B Model.

we prepare a variant VDS [sm-gt] [sm] to validate that the cost in computing similarity-based logits can be further optimized to $1/v$. It merely measures the similarity of the latent representation with one semantic basis, that is the corresponding ground truth (short as gt), instead of all semantic bases.

Logits Disentanglement. By amplifying and suppressing the logits values before loss computation, we can show the difference between entangled logits and disentangled logits, and further, reveal the effects of logits disentanglement. We take a simple strategy to manipulate the logits, that is, applying the natural exponential function (short as exp) to the logits, and then, normalizing the results. This operation amplifies the largest values and suppresses small values, while maintaining the magnitude relation of values. Therefore, we prepare such variants VDS [mm-exp] [sm] and VDS [sm-exp] [sm], for matrix multiplication and similarity measurement respectively.

Based on the results shown in Table 6, compared to the baseline approach VDS, both VDS [sm] [mm] and VDS [mm] [sm] show similar performance on average. The minor difference between the performance of VDS and two variantsmm indicates an almost equivalence of two practices of logits computation in LM forward-pass, in terms of the effects, no matter whether for either inference or clustering. It proves the correctness of our hypothesis on the correlations of the representations similarity and distribution similarity. Meanwhile, we found in some datasets (AGNews, SST5, WebSS), VDS [mm] [sm] performs not as good as the baseline, while in other datasets performs better. It indicates the two practices are not strictly equivalent, and their differences are more likely to cause slight differences in clustering than in inference. Further, we can know that cosine similarity may not be the optimal metric for similarity-based logits, if the two practices must be strictly equivalent.

In addition, the performance of VDS [sm-gt] [mm] is slightly better than that of VDS. This is because the variant is better utilizing the logits disentanglement to avoid the effects of these irrelevant semantic bases in clustering. Meanwhile, their computation costs differ a lot. Taking Llama3-8B as an example, the vocabulary size is 128256 and the dimension size is 4096, so each time of logits computation, we need to measure the similarity with all semantic bases. The required floating-point operations is 3.15×10^9 FLOPs. It is more costly than using matrix multiplication for logits computation, which only requires 1.05×10^9 FLOPs. In contrast, VDS [sm-gt] [mm] only measures the similarity with one semantic basis in logits computation, which only requires 2.46×10^4 FLOPs. It means a **five-order-of-magnitude** improvement in the computational cost in each logits computation, which is a huge computation advantage of similarity-based logits.

On logits disentanglement, compared with VDS [mm] [sm], the performance of VDS [mm-exp] [sm] shows a huge performance drop. In contrast, compared with VDS, the performance of VDS [sm-exp] [sm] is almost the same. The reason explaining the contrasting phenomena is the logits disentanglement. For matrix-multiplication logits, the logits is entangled so it is sensitive to the value differences on vocabulary labels. In contrast, for similarity-based logits, the logits is disentangled so it shows better robustness, and is insensitive to the value differences on vocabulary labels. A robust logits-numerical sensitivity supports direct and complex manipulations on the latent representations or even on the logits, since the loss computation is only sensitive to the relative magnitude for numeric values of logits, instead of the absolute magnitude.

6 Related Work

Generally, retrieval-augmented methods combine data retrieval and LM for better performance, such as in-context learning, which prompts LM with the retrieved task demonstrations. The demonstrations are in the form of an input-output pair, and will compose with the given input as the new input. The retrieval is conducted based on the similarity of the corpus data to the given input. Similarly, the

data to retrieve can be the context with the potentially related background. The general practice of similarity measurement in data retrieval is based on embeddings or representations, but KP evaluates the similarities of data based on the logits. Besides, KP retrieval the same amount of downstream data for each label in the vocabulary for a balance. Similar to retrieval-augmented methods, nearest-neighbor methods use the retrieval technique for improvements as well. However, it happens at the output side, such as the LM last-layer, instead of the input side. The data to retrieve is key-value pairs, for example, let the representation be the key and the corresponding ground truth be the value. The given representation is used as the query to retrieve the related history data. Then LM does inference with hybrid logits: one is from the model prediction while the other one is from the nearest-neighbor retrieval. The hybrid logits will be used to compute a normalized probability distribution. It has been used for language modeling in k NN-LM [38] and machine translation in k NN-MT [39]. A similar practice is using activations as the key [40]. A further topic along this direction is to realize retrieval-based neuro-symbolic inference, such as RETOMATON [41].

To reduce the computation cost of finetuning large-scale LMs, and the storage cost of the finetuned models, PEFT methods only update partial parameters. Compared with full parameter finetuning, PEFT methods can better avoid catastrophic forgetting [42], and learn better from a small amount of data. Adapter methods directly introduce new modules to the LMs, such as bottleneck adapters [43] and compacter [44]. PROMPT TUNING prepends tunable tokens to the input data. Similarly, PREFIX-TUNING modifies the multi-head attention with new parameters, that is, prepending trainable vectors to the key and value matrices. LORA [28] uses low-rank matrix to learn the additive updates on the self-attention weight matrix, while its variants are improving the parameter efficiency, such as ADALORA [45], DORA [46]. Similarly, OPT [47] uses orthogonal transformations to learn the multiplicative weight updates, and its variant BOFT [48] introduces factorization techniques for better parameter efficiency. While IA³ [29] rescales the activations by tuning additional coefficients. In addition, some work is the combinations of other PEFT methods [49]. For example, mix-and-match adapters are a combination of prefix-tuning and bottleneck adapters [50].

7 Conclusion

In this paper, we proposed a novel approach for in-context learning, “vocabulary-defined semantics”. It incorporates KNN decisions into LM inference to improve the performance. We define semantic bases, a collection of semantically equivalent representations to label space of language model, to define the semantic property of LM latent space. Leveraging the local isotropy of latent space, we propose similarity-based logits to quantify the semantic gap of the language model with downstream data. Further, we introduce a neural clustering module to optimize the logits, which in turn mitigates the semantic gap. Based on the results of extensive experiments, our semantic-based approach shows effectiveness and efficiency LM adaptation. It significantly outperforms the state-of-the-art, while showing advantages in both the computation cost and storage cost. Moreover, through our ablation study, similarity-based logits is as good as the multiplication-based logits computation, but performs better in numerical robustness. In the future, we will explore more topics where our semantic-based approach can help, contributing to not only LM performance, but also LM interpretability.

References

- [1] Rishi Bommasani, Drew A. Hudson, Ehsan Adeli, Russ Altman, Simran Arora, Sydney von Arx, Michael S. Bernstein, Jeannette Bohg, Antoine Bosselut, Emma Brunskill, Erik Brynjolfsson, S. Buch, Dallas Card, Rodrigo Castellon, Niladri S. Chatterji, Annie S. Chen, Kathleen A. Creel, Jared Davis, Dora Demszky, Chris Donahue, Moussa Doumbouya, Esin Durmus, Stefano Ermon, John Etchemendy, Kawin Ethayarajh, Li Fei-Fei, Chelsea Finn, Trevor Gale, Lauren Gillespie, Karan Goel, Noah D. Goodman, Shelby Grossman, Neel Guha, Tatsunori Hashimoto, Peter Henderson, John Hewitt, Daniel E. Ho, Jenny Hong, Kyle Hsu, Jing Huang, Thomas F. Icard, Saahil Jain, Dan Jurafsky, Pratyusha Kalluri, Siddharth Karamcheti, Geoff Keeling, Fereshthe Khani, O. Khattab, Pang Wei Koh, Mark S. Krass, Ranjay Krishna, Rohith Kuditipudi, Ananya Kumar, Faisal Ladhak, Mina Lee, Tony Lee, Jure Leskovec, Isabelle Levent, Xiang Lisa Li, Xuechen Li, Tengyu Ma, Ali Malik, Christopher D. Manning, Suvir Mirchandani, Eric Mitchell, Zanele Munyikwa, Suraj Nair, Avaniika Narayan, Deepak Narayanan, Benjamin Newman, Allen Nie, Juan Carlos Niebles, Hamed Nilforoshan, J. F. Nyarko, Giray Ogut, Laurel J. Orr, Isabel Papadimitriou, Joon Sung Park, Chris Piech, Eva Portelance, Christopher

- Potts, Aditi Raghunathan, Robert Reich, Hongyu Ren, Frieda Rong, Yusuf H. Roohani, Camilo Ruiz, Jack Ryan, Christopher R’e, Dorsa Sadigh, Shiori Sagawa, Keshav Santhanam, Andy Shih, Krishna Parasuram Srinivasan, Alex Tamkin, Rohan Taori, Armin W. Thomas, Florian Tramèr, Rose E. Wang, William Wang, Bohan Wu, Jiajun Wu, Yuhuai Wu, Sang Michael Xie, Michihiro Yasunaga, Jiaxuan You, Matei A. Zaharia, Michael Zhang, Tianyi Zhang, Xikun Zhang, Yuhui Zhang, Lucia Zheng, Kaitlyn Zhou, and Percy Liang. On the opportunities and risks of foundation models. *ArXiv*, abs/2108.07258, 2021.
- [2] Tianxiang Sun, Yunfan Shao, Hong Qian, Xuanjing Huang, and Xipeng Qiu. Black-box tuning for language-model-as-a-service. *ArXiv*, abs/2201.03514, 2022.
- [3] Qingxiu Dong, Lei Li, Damai Dai, Ce Zheng, Zhiyong Wu, Baobao Chang, Xu Sun, Jingjing Xu, and Zhifang Sui. A survey on in-context learning. 2022.
- [4] Jason Wei, Yi Tay, Rishi Bommasani, Colin Raffel, Barret Zoph, Sebastian Borgeaud, Dani Yogatama, Maarten Bosma, Denny Zhou, Donald Metzler, Ed Chi, Tatsunori Hashimoto, Oriol Vinyals, Percy Liang, Jeff Dean, and William Fedus. Emergent abilities of large language models. *ArXiv*, abs/2206.07682, 2022.
- [5] Ohad Rubin, Jonathan Herzig, and Jonathan Berant. Learning to retrieve prompts for in-context learning. *ArXiv*, abs/2112.08633, 2021.
- [6] Xiaonan Li, Kai Lv, Hang Yan, Tianya Lin, Wei Zhu, Yuan Ni, Guo Tong Xie, Xiaoling Wang, and Xipeng Qiu. Unified demonstration retriever for in-context learning. *ArXiv*, abs/2305.04320, 2023.
- [7] Jinghan Yang, Shuming Ma, and Furu Wei. Auto-icl: In-context learning without human supervision. *ArXiv*, abs/2311.09263, 2023.
- [8] Zhe Yang, Damai Dai, Peiyi Wang, and Zhifang Sui. Not all demonstration examples are equally beneficial: Reweighting demonstration examples for in-context learning. *ArXiv*, abs/2310.08309, 2023.
- [9] Yinpeng Liu, Jiawei Liu, Xiang Shi, Qikai Cheng, and Wei Lu. Let’s learn step by step: Enhancing in-context learning ability with curriculum learning. *ArXiv*, abs/2402.10738, 2024.
- [10] Qi Guo, Leiyu Wang, Yidong Wang, Wei Ye, and Shikun Zhang. What makes a good order of examples in in-context learning. In *Annual Meeting of the Association for Computational Linguistics*, 2024.
- [11] Benfeng Xu, Quan Wang, Zhendong Mao, Yajuan Lyu, Qiaoqiao She, and Yongdong Zhang. knn prompting: Beyond-context learning with calibration-free nearest neighbor inference. *ArXiv*, abs/2303.13824, 2023.
- [12] Alec Radford, Jeff Wu, Rewon Child, David Luan, Dario Amodei, and Ilya Sutskever. Language models are unsupervised multitask learners. 2019.
- [13] An Yang, Baosong Yang, Binyuan Hui, Bo Zheng, Bowen Yu, Chang Zhou, Chengpeng Li, Chengyuan Li, Dayiheng Liu, Fei Huang, Guanting Dong, Haoran Wei, Huan Lin, Jialong Tang, Jialin Wang, Jian Yang, Jianhong Tu, Jianwei Zhang, Jianxin Ma, Jin Xu, Jingren Zhou, Jinze Bai, Jinzheng He, Junyang Lin, Kai Dang, Keming Lu, Ke-Yang Chen, Kexin Yang, Mei Li, Min Xue, Na Ni, Pei Zhang, Peng Wang, Ru Peng, Rui Men, Ruize Gao, Runji Lin, Shijie Wang, Shuai Bai, Sinan Tan, Tianhang Zhu, Tianhao Li, Tianyu Liu, Wenbin Ge, Xiaodong Deng, Xiaohuan Zhou, Xingzhang Ren, Xinyu Zhang, Xipin Wei, Xuancheng Ren, Yang Fan, Yang Yao, Yichang Zhang, Yunyang Wan, Yunfei Chu, Zeyu Cui, Zhenru Zhang, and Zhi-Wei Fan. Qwen2 technical report. *ArXiv*, abs/2407.10671, 2024.
- [14] Gemma Team Morgane Riviere, Shreya Pathak, Pier Giuseppe Sessa, Cassidy Hardin, Surya Bhupatiraju, L’eonard Hussenot, Thomas Mesnard, Bobak Shahriari, Alexandre Ram’e, Johan Ferret, Peter Liu, Pouya Dehghani Tafti, Abe Friesen, Michelle Casbon, Sabela Ramos, Ravin Kumar, Charline Le Lan, Sammy Jerome, Anton Tsitsulin, Nino Vieillard, Piotr Stańczyk, Sertan Girgin, Nikola Momchev, Matt Hoffman, Shantanu Thakoor, Jean-Bastien Grill, Behnam Neyshabur, Alanna Walton, Aliaksei Severyn, Alicia Parrish, Aliya Ahmad, Allen Hutchison, Alvin Abdagic, Amanda Carl, Amy Shen, Andy Brock, Andy Coenen, Anthony Laforge, Antonia Paterson, Ben Bastian, Bilal Piot, Boxi Wu, Brandon Royal, Charlie Chen, Chintu Kumar, Chris Perry, Christoper A. Welty, Christopher A. Choquette-Choo, Danila Sinopalnikov, David Weinberger, Dimple Vijaykumar, Dominika Rogozińska, D. Herbison, Elisa Bandy, Emma Wang, Eric Noland, Erica Moreira, Evan Senter, Evgenii Eltyshev, Francesco Visin,

Gabriel Rasskin, Gary Wei, Glenn Cameron, Gus Martins, Hadi Hashemi, Hanna Klimczak-Plucińska, Harleen Batra, Harsh Dhand, Ivan Nardini, Jacinda Mein, Jack Zhou, James Svensson, Jeff Stanway, Jetha Chan, Jin Zhou, Joana Carrasqueira, Joana Iljazi, Jocelyn Becker, Joe Fernandez, Joost R. van Amersfoort, Josh Gordon, Josh Lipschultz, Joshua Newlan, Junsong Ji, Kareem Mohamed, Kartikeya Badola, Kat Black, Katie Millican, Keelin McDonell, Kelvin Nguyen, Kiranbir Sodhia, Kish Greene, Lars Lowe Sjoesund, Lauren Usui, L. Sifre, L. Heuermann, Leticia Lago, Lilly McNealus, Livio Baldini Soares, Logan Kilpatrick, Lucas Dixon, Luciano Martins, Machel Reid, Manvinder Singh, Mark Iverson, Martin Gorner, Mat Velloso, Mateo Wirth, Matt Davidow, Matt Miller, Matthew Rahtz, Matthew Watson, Meg Risdal, Mehran Kazemi, Michael Moynihan, Ming Zhang, Minsuk Kahng, Minwoo Park, Mofi Rahman, Mohit Khatwani, Natalie Dao, Nenshad Bardoliwalla, Nesh Devanathan, Neta Dumai, Nilay Chauhan, Oscar Wahltinez, Pankil Botarda, Parker Barnes, Paul Barham, Paul Michel, Pengchong Jin, Petko Georgiev, Phil Culliton, Pradeep Kuppala, Ramona Comanescu, Ramona Merhej, Reena Jana, Reza Rokni, Rishabh Agarwal, Ryan Mullins, Samaneh Saadat, S. Mc Carthy, Sarah Perrin, S'ebastien Arnold, Sebastian Krause, Shengyang Dai, Shruti Garg, Shruti Sheth, Sue Ronstrom, Susan Chan, Timothy Jordan, Ting Yu, Tom Eccles, Tom Hennigan, Tomás Kociský, Tulsee Doshi, Vihan Jain, Vikas Yadav, Vilobh Meshram, Vishal Dharmadhikari, Warren Barkley, Wei Wei, Wenming Ye, Woohyun Han, Woosuk Kwon, Xiang Xu, Zhe Shen, Zhitao Gong, Zichuan Wei, Victor Cotruta, Phoebe Kirk, Anand Rao, Minh Giang, Ludovic Peran, Tris Brian Warkentin, Eli Collins, Joelle Barral, Zoubin Ghahramani, Raia Hadsell, D. Sculley, Jeanine Banks, Anca Dragan, Slav Petrov, Oriol Vinyals, Jeffrey Dean, Demis Hassabis, Koray Kavukcuoglu, Clément Farabet, Elena Buchatskaya, Sebastian Borgeaud, Noah Fiedel, Armand Joulin, Kathleen Kenealy, Robert Dadashi, and Alek Andreev. Gemma 2: Improving open language models at a practical size. *ArXiv*, abs/2408.00118, 2024.

- [15] Abhimanyu Dubey, Abhinav Jauhri, Abhinav Pandey, Abhishek Kadian, Ahmad Al-Dahle, Aiesha Letman, Akhil Mathur, Alan Schelten, Amy Yang, Angela Fan, Anirudh Goyal, Anthony Hartshorn, Aobo Yang, Archi Mitra, Archie Sravankumar, Artem Korenev, Arthur Hinsvark, Arun Rao, Aston Zhang, Aurelien Rodriguez, Austen Gregerson, Ava Spataru, Baptiste Rozière, Bethany Biron, Binh Tang, Bobbie Chern, Charlotte Caucheteux, Chaya Nayak, Chloe Bi, Chris Marra, Chris McConnell, Christian Keller, Christophe Touret, Chunyang Wu, Corinne Wong, Cristian Cantón Ferrer, Cyrus Nikolaidis, Damien Allonsius, Daniel Song, Danielle Pintz, Danny Livshits, David Esibou, Dhruv Choudhary, Dhruv Mahajan, Diego Garcia-Olano, Diego Perino, Dieuwke Hupkes, Egor Lakomkin, Ehab A. AlBadawy, Elina Lobanova, Emily Dinan, Eric Michael Smith, Filip Radenovic, Frank Zhang, Gabriele Synnaeve, Gabrielle Lee, Georgia Lewis Anderson, Graeme Nail, Grégoire Mialon, Guanglong Pang, Guillem Cucurell, Hailey Nguyen, Hannah Korevaar, Hu Xu, Hugo Touvron, Iliyan Zarov, Imanol Arrieta Ibarra, Isabel M. Kloumann, Ishan Misra, Ivan Evtimov, Jade Copet, Jaewon Lee, Jan Laursen Geffert, Jana Vranes, Jason Park, Jay Mahadeokar, Jeet Shah, Jelmer van der Linde, Jennifer Billock, Jenny Hong, Jenya Lee, Jeremy Fu, Jianfeng Chi, Jianyu Huang, Jiawen Liu, Jie Wang, Jiecao Yu, Joanna Bitton, Joe Spisak, Jongsoo Park, Joseph Rocca, Joshua Johnstun, Joshua Saxe, Ju-Qing Jia, Kalyan Vasuden Alwala, K. Upasani, Kate Plawiak, Keqian Li, Ken-591 neth Heafield, Kevin Stone, Khalid El-Arini, Krithika Iyer, Kshitiz Malik, Kuenley Chiu, Kunal Bhalla, Lauren Rantala-Yearly, Laurens van der Maaten, Lawrence Chen, Liang Tan, Liz Jenkins, Louis Martin, Lovish Madaan, Lubo Malo, Lukas Blecher, Lukas Landzaat, Luke de Oliveira, Madeline C. Muzzi, Mahesh Babu Pasupuleti, Mannat Singh, Manohar Paluri, Marcin Kardas, Mathew Oldham, Mathieu Rita, Maya Pavlova, Melissa Hall Melanie Kambadur, Mike Lewis, Min Si, Mitesh Kumar Singh, Mona Hassan, Naman Goyal, Narjes Torabi, Nikolay Bashlykov, Nikolay Bogoychev, Niladri S. Chatterji, Olivier Duchenne, Onur cCelebi, Patrick Alrassy, Pengchuan Zhang, Pengwei Li, Petar Vasic, Peter Weng, Prajjwal Bhargava, Pratik Dubal, Praveen Krishnan, Punit Singh Koura, Puxin Xu, Qing He, Qingxiao Dong, Ragavan Srinivasan, Raj Ganapathy, Ramon Calderer, Ricardo Silveira Cabral, Robert Stojnic, Roberta Raileanu, Rohit Girdhar, Rohit Patel, Romain Sauvestre, Ronnie Polidoro, Roshan Sumbaly, Ross Taylor, Ruan Silva, Rui Hou, Rui Wang, Saghar Hosseini, Sahana Chennabasappa, Sanjay Singh, Sean Bell, Seohyun Sonia Kim, Sergey Edunov, Shaoliang Nie, Sharan Narang, Sharath Chandra Raparthy, Sheng Shen, Shengye Wan, Shruti Bhosale, Shun Zhang, Simon Vandenhende, Soumya Batra, Spencer Whitman, Sten Sootla, Stephane Collot, Suchin Gururangan, Sydney Borodinsky, Tamar Herman, Tara Fowler, Tarek Sheasha, Thomas Georgiou, Thomas Scialom, Tobias Speckbacher, Todor Mihaylov, Tong Xiao, Ujjwal Karn, Vedanuj Goswami, Vibhor Gupta, Vignesh Ramanathan, Viktor Kerkez, Vincent Gouguet,

Virginie Do, Vish Vogeti, Vladan Petrovic, Weiwei Chu, Wenhan Xiong, Wenyin Fu, Whitney Meers, Xavier Martinet, Xiaodong Wang, Xiaoqing Ellen Tan, Xinfeng Xie, Xuchao Jia, Xuewei Wang, Yaelle Goldschlag, Yashesh Gaur, Yasmine Babaei, Yiqian Wen, Yiwen Song, Yuchen Zhang, Yue Li, Yuning Mao, Zacharie Delpierre Coudert, Zhengxu Yan, Zhengxing Chen, Zoe Papakipos, Aaditya K. Singh, Aaron Grattafiori, Abha Jain, Adam Kelsey, Adam Shajnfeld, Adi Gangidi, Adolfo Victoria, Ahuva Goldstand, Ajay Menon, Ajay Sharma, Alex Boesenberg, Alex Vaughan, Alexei Baevski, Allie Feinstein, Amanda Kallet, Amit Sangani, Anam Yunus, Andrei Lupu, Andres Alvarado, Andrew Caples, Andrew Gu, Andrew Ho, Andrew Poulton, Andrew Ryan, Ankit Ramchandani, Annie Franco, Aparajita Saraf, Arkabandhu Chowdhury, Ashley Gabriel, Ashwin Bharambe, Assaf Eisenman, Azadeh Yazdan, Beau James, Ben Maurer, Ben Leonhardi, Bernie Huang, Beth Loyd, Beto De Paola, Bhargavi Paranjape, Bing Liu, Bo Wu, Boyu Ni, Braden Hancock, Bram Wasti, Brandon Spence, Brani Stojkovic, Brian Gamido, Britt Montalvo, Carl Parker, Carly Burton, Catalina Mejia, Changhan Wang, Changkyu Kim, Chao Zhou, Chester Hu, Ching-Hsiang Chu, Chris Cai, Chris Tindal, Christoph Feichtenhofer, Damon Civin, Dana Beaty, Daniel Kreymer, Shang-Wen Li, Danny Wyatt, David Adkins, David Xu, Davide Testuggine, Delia David, Devi Parikh, Diana Liskovich, Didem Foss, DingKang Wang, Duc Le, Dustin Holland, Edward Dowling, Eissa Jamil, Elaine Montgomery, Eleonora Presani, Emily Hahn, Emily Wood, Erik Brinkman, Esteban Arcaute, Evan Dunbar, Evan Smothers, Fei Sun, Felix Kreuk, Feng Tian, Firat Ozgenel, Francesco Caggioni, Francisco Guzm'an, Frank J. Kanayet, Frank Seide, Gabriela Medina Florez, Gabriella Schwarz, Gada Badeer, Georgia Swee, Gil Halpern, Govind Thattai, Grant Herman, Grigory G. Sizov, Guangyi Zhang, Guna Lakshminarayanan, Hamid Shojanazeri, Han Zou, Hannah Wang, Han Zha, Haroun Habeeb, Harrison Rudolph, Helen Suk, Henry Aspegren, Hunter Goldman, Igor Molybog, Igor Tufanov, Irina-Elena Veliche, Itai Gat, Jake Weissman, James Geboski, James Kohli, Japhet Asher, Jean-Baptiste Gaya, Jeff Marcus, Jeff Tang, Jennifer Chan, Jenny Zhen, Jeremy Reizenstein, Jeremy Teboul, Jessica Zhong, Jian Jin, Jingyi Yang, Joe Cummings, Jon Carvill, Jon Shepard, Jonathan McPhie, Jonathan Torres, Josh Ginsburg, Junjie Wang, Kaixing(Kai) Wu, U KamHou, Karan Saxena, Karthik Prasad, Kartikay Khandelwal, Katayoun Zand, Kathy Matosich, Kaushik Veeraraghavan, Kelly Michelena, Keqian Li, Kun Huang, Kunal Chawla, Kushal Lakhota, Kyle Huang, Lailin Chen, Lakshya Garg, A Lavender, Leandro Silva, Lee Bell, Lei Zhang, Liangpeng Guo, Licheng Yu, Liron Moshkovich, Luca Wehrstedt, Madian Khabsa, Manav Avalani, Manish Bhatt, Maria Tsimpoukelli, Martynas Mankus, Matan Hasson, Matthew Lennie, Matthias Reso, Maxim Groshev, Maxim Naumov, Maya Lathi, Meghan Keneally, Michael L. Seltzer, Michal Valko, Michelle Restrepo, Mihir Patel, Mik Vyatskov, Mikayel Samvelyan, Mike Clark, Mike Macey, Mike Wang, Miquel Jubert Hermoso, Mo Metanat, Mohammad Rastegari, Munish Bansal, Nandhini Santhanam, Natascha Parks, Natasha White, Navyata Bawa, Nayan Singhal, Nick Egebo, Nicolas Usunier, Nikolay Pavlovich Laptev, Ning Dong, Ning Zhang, Norman Cheng, Oleg Chernoguz, Olivia Hart, Omkar Salpekar, Ozlem Kalinli, Parkin Kent, Parth Parekh, Paul Saab, Pavan Balaji, Pedro Rittner, Philip Bontrager, Pierre Roux, Piotr Dollár, Polina Zvyagina, Prashant Ratanchandani, Pritish Yuvraj, Qian Liang, Rachad Alao, Rachel Rodriguez, Rafi Ayub, Raghotham Murthy, Raghu Nayani, Rahul Mitra, Raymond Li, Rebekkah Hogan, Robin Battey, Rocky Wang, Rohan Maheswari, Russ Howes, Ruty Rinott, Sai Jayesh Bondu, Samyak Datta, Sara Chugh, Sara Hunt, Sargun Dhillon, Sasha Sidorov, Satadru Pan, Saurabh Verma, Seiji Yamamoto, Sharadh Ramaswamy, Shaun Lindsay, Sheng Feng, Shenghao Lin, Shengxin Cindy Zha, Shiva Shankar, Shuqiang Zhang, Sinong Wang, Sneha Agarwal, Soji Sajuyigbe, Soumith Chintala, Stephanie Max, Stephen Chen, Steve Kehoe, Steve Satterfield, Sudarshan Govindaprasad, Sumit Gupta, Sung-Bae Cho, Sunny Virk, Suraj Subramanian, Sy Choudhury, Sydney Goldman, Tal Remez, Tamar Glaser, Tamara Best, Thilo Kohler, Thomas Robinson, Tianhe Li, Tianjun Zhang, Tim Matthews, Timothy Chou, Tzook Shaked, Varun Vontimitta, Victoria Ajayi, Victoria Montanez, Vijai Mohan, Vinay Satish Kumar, Vishal Mangla, Vlad Ionescu, Vlad Andrei Poenaru, Vlad T. Mihailescu, Vladimir Ivanov, Wei Li, Wenchen Wang, Wenwen Jiang, Wes Bouaziz, Will Constable, Xia Tang, Xiaofang Wang, Xiaoqian Wu, Xiaolan Wang, Xide Xia, Xilun Wu, Xinbo Gao, Yanjun Chen, Ye Hu, Ye Jia, Ye Qi, Yenda Li, Yilin Zhang, Ying Zhang, Yossi Adi, Youngjin Nam, Yu Wang, Yuchen Hao, Yundi Qian, Yuzi He, Zach Rait, Zachary DeVito, Zef Rosnbrick, Zhaoduo Wen, Zhenyu Yang, and Zhiwei Zhao. The llama 3 herd of models. *ArXiv*, abs/2407.21783, 2024.

- [16] Irina Higgins, David Amos, David Pfau, Sébastien Racanière, Loïc Matthey, Danilo Jimenez Rezende, and Alexander Lerchner. Towards a definition of disentangled representations. *ArXiv*, abs/1812.02230, 2018.

- [17] Xingyu Cai, Jiaji Huang, Yu-Lan Bian, and Kenneth Ward Church. Isotropy in the contextual embedding space: Clusters and manifolds. In *International Conference on Learning Representations*, 2021.
- [18] Jie Hu, Li Shen, Samuel Albanie, Gang Sun, and Enhua Wu. Squeeze-and-excitation networks. *2018 IEEE/CVF Conference on Computer Vision and Pattern Recognition*, pages 7132–7141, 2017.
- [19] Xiang Zhang, Junbo Jake Zhao, and Yann LeCun. Character-level convolutional networks for text classification. In *Neural Information Processing Systems*, 2015.
- [20] Bo Pang and Lillian Lee. A sentimental education: Sentiment analysis using subjectivity summarization based on minimum cuts. *ArXiv*, cs.CL/0409058, 2004.
- [21] Ellen M. Voorhees and Dawn M. Tice. Building a question answering test collection. In *Annual International ACM SIGIR Conference on Research and Development in Information Retrieval*, 2000.
- [22] Xuan Hieu Phan, Minh Le Nguyen, and Susumu Horiguchi. Learning to classify short and sparse text & web with hidden topics from large-scale data collections. In *The Web Conference*, 2008.
- [23] Bo Pang and Lillian Lee. Seeing stars: Exploiting class relationships for sentiment categorization with respect to rating scales. In *Annual Meeting of the Association for Computational Linguistics*, 2005.
- [24] Richard Socher, Alex Perelygin, Jean Wu, Jason Chuang, Christopher D. Manning, A. Ng, and Christopher Potts. Recursive deep models for semantic compositionality over a sentiment treebank. In *Conference on Empirical Methods in Natural Language Processing*, 2013.
- [25] Elvis Saravia, Hsien-Chi Toby Liu, Yen-Hao Huang, Junlin Wu, and Yi-Shin Chen. Carer: Contextualized affect representations for emotion recognition. In *Conference on Empirical Methods in Natural Language Processing*, 2018.
- [26] William B. Dolan and Chris Brockett. Automatically constructing a corpus of sentential paraphrases. In *International Joint Conference on Natural Language Processing*, 2005.
- [27] Sewon Min, Xinxu Lyu, Ari Holtzman, Mikel Artetxe, Mike Lewis, Hannaneh Hajishirzi, and Luke Zettlemoyer. Rethinking the role of demonstrations: What makes in-context learning work? *ArXiv*, abs/2202.12837, 2022.
- [28] J. Edward Hu, Yelong Shen, Phillip Wallis, Zeyuan Allen-Zhu, Yuanzhi Li, Shean Wang, and Weizhu Chen. Lora: Low-rank adaptation of large language models. *ArXiv*, abs/2106.09685, 2021.
- [29] Haokun Liu, Derek Tam, Mohammed Muqeeth, Jay Mohta, Tenghao Huang, Mohit Bansal, and Colin Raffel. Few-shot parameter-efficient fine-tuning is better and cheaper than in-context learning. *ArXiv*, abs/2205.05638, 2022.
- [30] Adam Paszke, Sam Gross, Francisco Massa, Adam Lerer, James Bradbury, Gregory Chanan, Trevor Killeen, Zeming Lin, Natalia Gimelshein, Luca Antiga, Alban Desmaison, Andreas Köpf, Edward Yang, Zach DeVito, Martin Raison, Alykhan Tejani, Sasank Chilamkurthy, Benoit Steiner, Lu Fang, Junjie Bai, and Soumith Chintala. Pytorch: An imperative style, high-performance deep learning library. In *Neural Information Processing Systems*, 2019.
- [31] Thomas Wolf, Lysandre Debut, Victor Sanh, Julien Chaumond, Clement Delangue, Anthony Moi, Pierric Cistac, Tim Rault, Rémi Louf, Morgan Funtowicz, and Jamie Brew. Transformers: State-of-the-art natural language processing. In *Conference on Empirical Methods in Natural Language Processing*, 2019.
- [32] Tim Dettmers, Artidoro Pagnoni, Ari Holtzman, and Luke Zettlemoyer. Qlora: Efficient finetuning of quantized llms. *ArXiv*, abs/2305.14314, 2023.
- [33] Xiaoxia Wu, Cheng Li, Reza Yazdani Aminabadi, Zhewei Yao, and Yuxiong He. Understanding int4 quantization for language models: Latency speedup, composability, and failure cases. In *International Conference on Machine Learning*, 2023.
- [34] Mor Geva, R. Schuster, Jonathan Berant, and Omer Levy. Transformer feed-forward layers are key-value memories. *ArXiv*, abs/2012.14913, 2020.

- [35] Mor Geva, Avi Caciularu, Ke Wang, and Yoav Goldberg. Transformer feed-forward layers build predictions by promoting concepts in the vocabulary space. *ArXiv*, abs/2203.14680, 2022.
- [36] Michael Hassid, Hao Peng, Daniel Rotem, Jungo Kasai, Ivan Montero, Noah A. Smith, and Roy Schwartz. How much does attention actually attend? questioning the importance of attention in pretrained transformers. In *Conference on Empirical Methods in Natural Language Processing*, 2022.
- [37] Aston Zhang, Yi Tay, Shuai Zhang, Alvin Chan, Anh Tuan Luu, Siu Cheung Hui, and Jie Fu. Beyond fully-connected layers with quaternions: Parameterization of hypercomplex multiplications with $1/n$ parameters. *ArXiv*, abs/2102.08597, 2021.
- [38] Urvashi Khandelwal, Omer Levy, Dan Jurafsky, Luke Zettlemoyer, and Mike Lewis. Generalization through memorization: Nearest neighbor language models. *ArXiv*, abs/1911.00172, 2020.
- [39] Urvashi Khandelwal, Angela Fan, Dan Jurafsky, Luke Zettlemoyer, and Mike Lewis. Nearest neighbor machine translation. *ArXiv*, abs/2010.00710, 2021.
- [40] Edouard Grave, Armand Joulin, and Nicolas Usunier. Improving neural language models with a continuous cache. *ArXiv*, abs/1612.04426, 2017.
- [41] Uri Alon, Frank F. Xu, Junxian He, Sudipta Sengupta, Dan Roth, and Graham Neubig. Neuro-symbolic language modeling with automaton-augmented retrieval. In *International Conference on Machine Learning*, 2022.
- [42] Ian J. Goodfellow, Mehdi Mirza, Xia Da, Aaron C. Courville, and Yoshua Bengio. An empirical investigation of catastrophic forgetting in gradient-based neural networks. *CoRR*, abs/1312.6211, 2013.
- [43] Neil Houlsby, Andrei Giurgiu, Stanislaw Jastrzebski, Bruna Morrone, Quentin de Laroussilhe, Andrea Gesmundo, Mona Attariyan, and Sylvain Gelly. Parameter-efficient transfer learning for nlp. *ArXiv*, abs/1902.00751, 2019.
- [44] Joe Davison. Compacter: Efficient low-rank hypercomplex adapter layers. In *Neural Information Processing Systems*, 2021.
- [45] Qingru Zhang, Minshuo Chen, Alexander W. Bukharin, Nikos Karampatziakis, Pengcheng He, Yu Cheng, Weizhu Chen, and Tuo Zhao. Adalora: Adaptive budget allocation for parameter-efficient fine-tuning. 2023.
- [46] Shih yang Liu, Chien-Yi Wang, Hongxu Yin, Pavlo Molchanov, Yu-Chiang Frank Wang, Kwang-Ting Cheng, and Min-Hung Chen. Dora: Weight-decomposed low-rank adaptation. *ArXiv*, abs/2402.09353, 2024.
- [47] Zeju Qiu, Wei yu Liu, Haiwen Feng, Yuxuan Xue, Yao Feng, Zhen Liu, Dan Zhang, Adrian Weller, and Bernhard Scholkopf. Controlling text-to-image diffusion by orthogonal finetuning. *ArXiv*, abs/2306.07280, 2023.
- [48] Weiyang Liu, Zeju Qiu, Yao Feng, Yuliang Xiu, Yuxuan Xue, Longhui Yu, Haiwen Feng, Zhen Liu, Juyeon Heo, Songyou Peng, Yandong Wen, Michael J. Black, Adrian Weller, and Bernhard Schölkopf. Parameter-efficient orthogonal finetuning via butterfly factorization. *ArXiv*, abs/2311.06243, 2023.
- [49] Yuning Mao, Lambert Mathias, Rui Hou, Amjad Almahairi, Hao Ma, Jiawei Han, Wen tau Yih, and Madian Khabza. Unipelt: A unified framework for parameter-efficient language model tuning. In *Annual Meeting of the Association for Computational Linguistics*, 2021.
- [50] Junxian He, Chunting Zhou, Xuezhe Ma, Taylor Berg-Kirkpatrick, and Graham Neubig. Towards a unified view of parameter-efficient transfer learning. *ArXiv*, abs/2110.04366, 2021.
- [51] Yao Lu, Max Bartolo, Alastair Moore, Sebastian Riedel, and Pontus Stenetorp. Fantastically ordered prompts and where to find them: Overcoming few-shot prompt order sensitivity. *ArXiv*, abs/2104.08786, 2021.
- [52] Georgios Arvanitidis, Lars Kai Hansen, and Søren Hauberg. Latent space oddity: on the curvature of deep generative models. *arXiv: Machine Learning*, 2017.

A Implementation Details

A.1 Prompt Templates

The prompt templates follow the practice of prior work [51], as shown in Table 7.

Dataset	Prompt	Label Space
AGNews	<i>Input:</i> Nets get Carter from Raptors. "INDIANAPOLIS – All-Star Vince Carter was traded by the Toronto Raptors to the New Jersey Nets for Alonzo Mourning, Eric Williams, Aaron Williams, and a pair of first-round draft picks yesterday." <i>Type:</i> business	world, sports, business, technology
CARER	<i>message:</i> i know a lot but i feel so stupid because i can not portray it <i>emotion:</i> sadness	sadness, joy, love, anger, fear, surprise
MR	<i>review:</i> "provides a porthole into that noble , trembling incoherence that defines us all ." <i>sentiment:</i> positive	negative, positive
MRPC	<i>Premise:</i> The 30-year bond US30YT = RR rose 22 / 32 for a yield of 4.31 percent , versus 4.35 percent at Wednesday 's close . <i>Hypothesis:</i> The 30-year bond US30YT = RR grew 1-3 / 32 for a yield of 4.30 percent , down from 4.35 percent late Wednesday . <i>Prediction:</i> not equivalent	equivalent, not equivalent
SST5	<i>review:</i> a deliciously nonsensical comedy about a city coming apart at its seams . <i>sentiment:</i> great	terrible, bad, okay, good, great
SUBJ	<i>input:</i> "looking for a short cut to fame , glass concocted sources , quotes and even entire stories , but his deception did not go unnoticed forever , and eventually , his world came crumbling down . . ." <i>type:</i> objective	subjective, objective
TREC	<i>Question:</i> What currency is used in Australia ? <i>Type:</i> entity	description, entity, expression, human, location, number
WebSS	<i>input:</i> americangymnasticsclub american gymnastic club recreational gymnastics boys girls schedule fees programs calendar birthday parties camps staff <i>type:</i> sports	business, computers, culture-arts-entertainment, education-science, engineering, health, politics-society, sports

TABLE 7: Prompt Template and Label Space in the Experiments.

A.2 Hyperparameters

In the demonstration retrieval, we randomly sample data from the training set. Following the practice of KP, we compute the maximum allowed number of demonstrations by setting the threshold of the truncation probability to be 5%. We stabilize the experiments using the default random seed 42.

In the clustering process of our approach VDS, since the neural clustering module is outside language models and directly working on the detached latent representations, we take large hyperparameters to speedup semantic clustering: the epoch number is 100 and the batch size is 256.

In the learning process of PEFT methods, we follow the recommended practices of LORA and IA³ based on their papers. That is, making the query-key-value matrices trainable in LORA, and also making the second fully-connected layer in the feed-forward module trainable in IA³. We take the commonly used hyperparameters, keeping the epoch number 1 and the batch size 1.

B More Discussion

B.1 General Semantic Basis

Considering the semantic basis is based on the LM vocabulary, we can duplicate the practice on the LM last-layer (after the last-layer, before LM-head) to the LM embedding-layer (after the embedding layer, before the first-layer) as well. For the sake of the opposite computation direction of representation, the semantic basis can be obtained by a matrix multiplication between onehot embedding and the embedding matrix. That is, we multiply the onehot embedding \vec{e} by the embedding matrix \mathbb{W} to obtain the corresponding representation \vec{r} . Expressed in formula, that is, $\vec{r} = \vec{e} \cdot \mathbb{W}$.

B.2 Disentanglement in Latent Space

The insights motivating *vocabulary-defined semantics* is logits disentanglement. In our approach, we compute logits *before* the LM-head, instead of *after*. Therefore, we can obtain the disentangled logits in latent space. In the latent space, the disentangled logits are useful to evaluate and optimize latent representations. Our approach is leveraging the vocabulary to define the semantics of last-layer latent space, therefore, we mainly guarantee the usefulness in the LM last-layer.

C More Results and Analysis

C.1 Quality of Latent Space Clustering

Dataset	Metric	GPT2				Qwen2			Gemma2		Llama3
		Small	Medium	Large	XL	0.5B	1.5B	7B	2B	9B	8B
AGNews	ARI [w/o]	0.306	0.285	0.351	0.265	0.145	0.425	0.528	0.000	0.000	0.402
	ARI [w/]	0.798	0.811	0.822	0.822	0.764	0.844	0.847	0.772	0.773	0.851
CARER	ARI [w/o]	0.015	0.015	0.033	0.096	0.153	0.135	0.236	0.037	0.018	0.172
	ARI [w/]	0.426	0.407	0.377	0.430	0.595	0.485	0.539	0.458	0.412	0.429
MR	ARI [w/o]	0.049	0.041	0.382	0.316	0.245	0.179	0.565	0.000	0.029	0.416
	ARI [w/]	0.384	0.502	0.514	0.536	0.494	0.649	0.734	0.224	0.203	0.659
MRPC	ARI [w/o]	0.000	0.000	0.000	0.000	0.000	-0.002	0.000	0.000	0.000	-0.002
	ARI [w/]	0.114	0.110	0.119	0.096	0.098	0.269	0.369	0.106	0.088	0.139
SST5	ARI [w/o]	0.022	0.018	0.004	0.009	0.052	0.030	0.244	0.004	0.000	0.018
	ARI [w/]	0.106	0.162	0.154	0.169	0.162	0.192	0.247	0.054	0.072	0.196
SUBJ	ARI [w/o]	0.001	0.121	0.013	0.000	0.028	0.025	0.087	0.009	0.030	0.194
	ARI [w/]	0.684	0.714	0.741	0.792	0.727	0.817	0.841	0.621	0.656	0.848
TREC	ARI [w/o]	0.100	0.074	0.151	0.070	0.292	0.083	0.138	0.003	0.000	0.183
	ARI [w/]	0.767	0.837	0.836	0.879	0.826	0.882	0.907	0.752	0.761	0.862
WebSS	ARI [w/o]	0.171	0.202	0.207	0.210	0.050	0.104	0.214	0.050	0.019	0.191
	ARI [w/]	0.578	0.606	0.590	0.620	0.579	0.638	0.667	0.475	0.457	0.666

TABLE 8: LM Performance w/ and w/o Semantic Clustering.

We can measure the quality of representation clustering via clustering metrics, such as *Adjusted Rand Index (ARI)*. The computation mechanism revolves around pairwise comparisons on clusterings. ARI measures how similar two clusterings are in each comparison, while accounting for the possibility of random agreement. The value range is $[-1, 1]$, the larger, the better. A value 0 or values close to 0 indicate a normal disordered situation.

The results are shown in Table 8, where we use labels in the form of `metric[identifier]` to mark variants, and identifier is either *w/o* or *w/*, representing whether semantic clustering is applied. We can see that semantic clustering can bring obvious improvements in the clustering quality.

C.2 Benefits of Semantic Clustering to KNN Decision

Dataset	Parameter	GPT2				Qwen2			Gemma2		Llama3
		Small	Medium	Large	XL	0.5B	1.5B	7B	2B	9B	8B
AGNews (Acc.)	k=1 [w/o]	0.704	0.721	0.759	0.760	0.578	0.721	0.739	0.576	0.514	0.795
	k=1 [w/]	0.915	0.918	0.925	0.928	0.898	0.935	0.938	0.909	0.898	0.940
	k=16 [w/o]	0.819	0.816	0.846	0.845	0.703	0.833	0.851	0.748	0.708	0.881
	k=16 [w/]	0.919	0.924	0.929	0.929	0.904	0.937	0.939	0.908	0.908	0.941
	k=256 [w/o]	0.852	0.855	0.876	0.875	0.760	0.861	0.886	0.825	0.817	0.899
	k=256 [w/]	0.919	0.924	0.929	0.929	0.903	0.938	0.939	0.909	0.908	0.941
WebSS (F1)	k=1 [w/o]	0.239	0.273	0.397	0.372	0.326	0.329	0.282	0.220	0.202	0.359
	k=1 [w/]	0.682	0.703	0.694	0.702	0.688	0.718	0.723	0.632	0.636	0.726
	k=16 [w/o]	0.345	0.413	0.592	0.580	0.493	0.506	0.465	0.290	0.249	0.537
	k=16 [w/]	0.691	0.711	0.701	0.709	0.695	0.736	0.728	0.638	0.653	0.730
	k=256 [w/o]	0.560	0.601	0.738	0.730	0.634	0.686	0.638	0.468	0.362	0.709
	k=256 [w/]	0.796	0.803	0.794	0.804	0.787	0.818	0.837	0.730	0.727	0.831

TABLE 9: LM Performance with k Nearest-Neighbor Methods.

Since the clustering quality is promoted by semantic clustering, we can anticipate that, the performance of the KNN decision will also be benefited. That is, our approach incorporates an improved

KNN decision process into LM inference. For ease of description, we use “sibling” to describe data representations that correspond to the same label in the vocabulary, and use “neighbor” to describe data representations that are close to each other in latent space. In semantic clustering, for each data, its siblings shall gradually become its neighbors.

We experimented with semantic clustering to validate its effects on nearest-neighbor methods, that is, predicting the class of data representations with the reference to the nearest neighboring data in the latent space. As shown in Table 9, there are obvious improvements in the performance when we apply semantic clustering. When the neighboring number k increased from $k = 1$ to $k = 256$, the performance of [w/o] is gradually increased and becomes closer to that of [w/]. The accuracy changes shown on [w/o] mean, that semantic clustering transforms the representations to make more neighboring data be the sibling data, which fulfills the expectation.

D Representations in Latent Space

To illustrate the effects of semantic clustering, we visualize latent representations of language models from different families using tSNE [52], mainly on the AGNews dataset. For example, as shown in Figure 2, before clustering, the data representations were messily scattered. In contrast, after clustering, the representations scatter into a few clusters, and in each cluster, the representations correspond to the same semantic meaning. By comparing the scattering situations of latent representations of different models before clustering, we can see the scattering situation of Gemma2-9B is the worst while that of Llama3-8B is the best, as shown in Figure 4 and Figure 5. It indicates the effects of semantic clustering may be larger on Gemma2-9B but smaller on Llama3-8B. Further, by comparing the scattering situations after clustering, we can see GPT2-XL, Qwen-7B, and Llama3-8B share a similar pattern, where all clusterings are spreading areas and are well distinguished. In contrast, in the case of Gemma2-9B, the latent representations are gathered as twisted curves, even though the curves are still well distinguished. The changes made by semantic clustering on latent representations illustrate the effects of our approach in in-context learning, and also explain why the improvements are significant on Gemma2 models while marginal on Llama3.

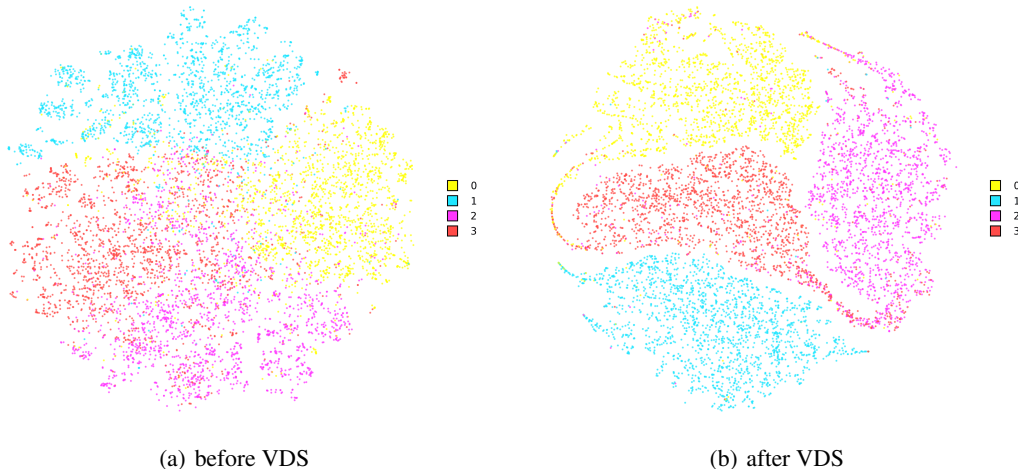


Figure 2: tSNE Illustration of latent space clustering on AGNews with GPT2-XL.

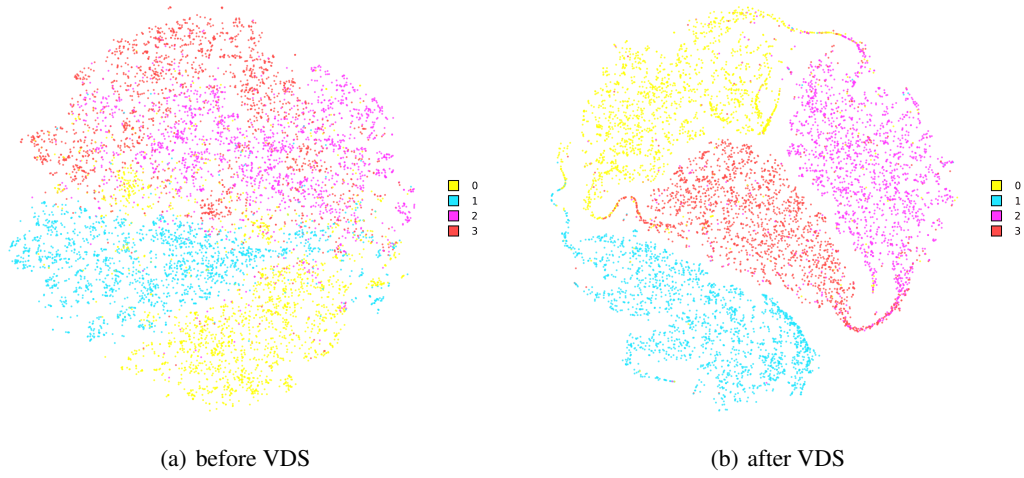


Figure 3: tSNE Illustration of latent space clustering on AGNews with Qwen-7B.

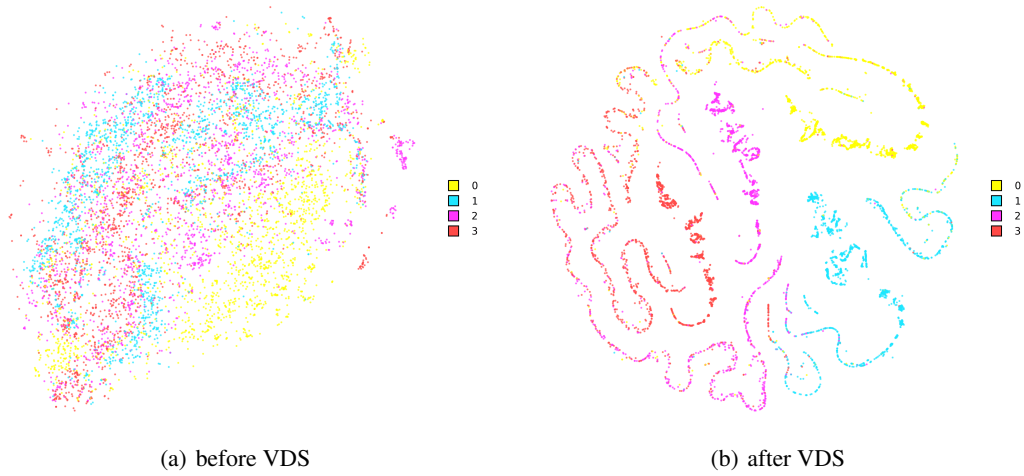


Figure 4: tSNE Illustration of latent space clustering on AGNews with Gemma2-9B.

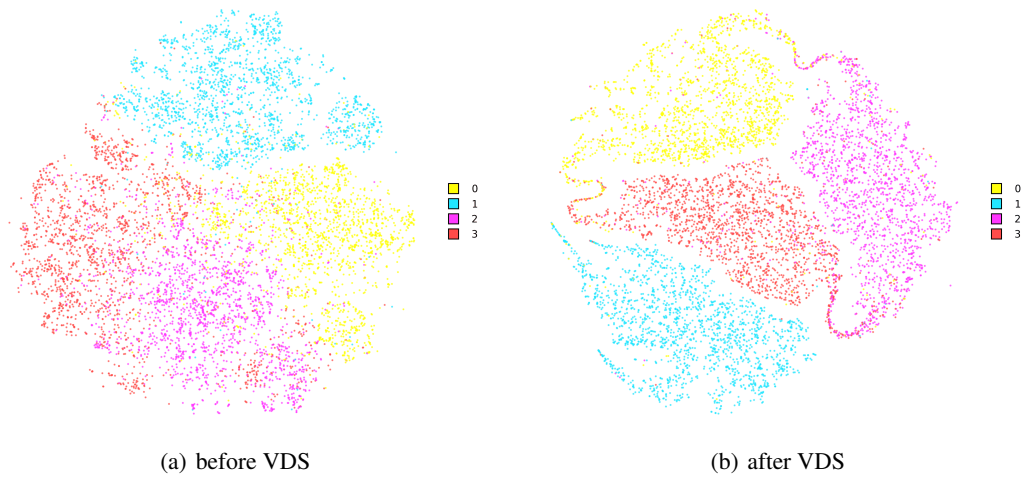


Figure 5: tSNE Illustration of latent space clustering on AGNews with Llama3-8B.